Ferromagnetic proximity effect in a-Co_xSi_{1-x}/Nb bilayers: Role of magnetic disorder and interface transparency

A. Alija,[1] D. Pérez de Lara,[2,3] E. M. Gonzalez,[3] G. N. Kakazei,[4,5] J. B. Sousa,[4] J. P. Araujo,[4] A. Hierro-Rodriguez,[1] J. I. Martín,[1] J. M. Alameda,[1] M. Vélez,[1,*] and J. L. Vicent[2,3]

[1]*Depto. Física, Universidad de Oviedo-CINN, 33007 Oviedo, Spain*

[2]*IMDEA-Nanociencia, Cantoblanco, 28049 Madrid, Spain*

[3]*Depto. Física de Materiales, Universidad Complutense de Madrid, 28040 Madrid, Spain*

[4]*IFIMUP and IN-Institute of Nanoscience and Nanotechnology, Departamento de Física da Faculdade de Ciências, Universidade do Porto, 4169-007 Porto, Portugal*

[5]*Institute of Magnetism, NAS of Ukraine, 36b Vernadskogo Boulevard, 03142 Kiev, Ukraine*

(Received 16 July 2010; revised manuscript received 26 October 2010; published 19 November 2010)

The superconducting and magnetic properties of a-Co_xSi_{1-x}/Nb bilayers have been studied as a function of Co content in order to analyze the superconducting/ferromagnetic proximity effect in a system with strong disorder in the magnetic layers. As Co atoms become more diluted, the magnetization of the amorphous a-Co_xSi_{1-x} alloy decreases gradually, whereas their resistivity increases and enters in a weak localization regime. The superconducting transition temperatures of the a-Co_xSi_{1-x}/Nb bilayers follow a decreasing trend as Co content is reduced, reaching the lowest value at the boundary between the ferromagnetic-nonmagnetic amorphous phases. These results can be understood in terms of the increase in interface transparency together with the changes in the spin-flip scattering term as magnetic disorder increases and the amorphous a-Co_xSi_{1-x} layers loose their magnetic character.

DOI: 10.1103/PhysRevB.82.184529 PACS number(s): 74.45.+c

I. INTRODUCTION

Superconductivity (S) and magnetism are, in general, antagonistic phenomena that can only coexist under very restricted conditions.[1] The study of hybrid structures, such as superconducting/magnetic multilayers,[2–8] superconducting/magnetic/superconducting junctions,[9] or superconducting magnetic nanostructures,[10] has revealed many remarkable phenomena such as direct and inverse proximity effect,[11] reentrant superconductivity[12] and critical temperature oscillations, or infinite magnetoresistance in superconducting spin valves.[13,14] Active theoretical work[15–22] in this field is helping to disentangle the subtle interplay between superconductivity and magnetism, depending on the different structural parameters of the superconducting/ferromagnetic (F) materials and the oscillating behavior of the superconducting order parameter within the ferromagnetic layers.

Some of the factors that emerge as crucial in determining the proximity effect in a particular S/F system are the strength of magnetic order and interface characteristics.[23] For example, several studies have analyzed the role of interface characteristics in S/F proximity effects by working with S/N/F structures in which a thin layer of normal metal is introduced in between the S and F materials[24–28] or changing surface geometry in nanostructured hybrids.[29] Also, the length scale for saturation of the proximity effect depends on the ferromagnetic layer: it changes from the range 0.1–1 nm in strong ferromagnets[4] such as Fe or Co to the range 1–10 nm in weak ferromagnets, such as Cu-Ni and Cu-Pd alloys.[5,30] This reflects the increase in the ferromagnetic coherence length ξ_F as magnetic order becomes weaker. However, the behavior of S/F hybrids is often much more complex: for example, an enhanced superconducting transition was observed in Nb/Fe/Cu multilayers when the Curie temperature of the Fe layer increased from 250 to 1000 K as a result of a fcc-bcc structural transition[31] and, in V/Fe_xV_{1-x} multilayers, the proximity effect presents a nonmonotonous dependence on iron content[23] that has been attributed to changes in interface transparency due to band mismatch at the V/Fe interface[14] as a result of exchange splitting in the ferromagnet.

Very recently, several theoretical works[32,33] have pointed to the relevance of disorder and inhomogeneities in the magnetic structure[34] within the magnetic layer at different length scales. However, most experimental works in F/S structures have been performed in epitaxial and polycrystalline multilayers and very little attention has been paid to amorphous materials[35] with a correlation length for disorder that can be comparable or even smaller than the ferromagnetic ξ_F length.

In this work, the superconducting and magnetic properties of a series of a-Co_xSi_{1-x}/Nb bilayers have been studied as a function of Co content. The structural characterization of these alloys[36–38] shows an amorphous structure for x below 0.75 with a certain degree of Co clustering that could provide the disordered Zeeman field analyzed in the proximity effect model by Ivanov *et al.*[33] The proximity effect is weak for high Co content but is enhanced at the boundary between the ferromagnetic-nonmagnetic amorphous phases. This behavior can be understood in terms of the interplay between interface transparency and spin-flip scattering by magnetic disorder as the magnetic character of the amorphous Co-Si alloy layer is gradually lost.

II. EXPERIMENTAL

Two series of samples have been used in this work: first, a set of 40-nm-thick Co_xSi_{1-x} films with Co concentration x in the range $x=0.78-0.56$ for the characterization of the mag-

netic and structural properties and, second, a set of 40 nm Co_xSi_{1-x}/25 nm Nb bilayers for the proximity effect measurements. The Co_xSi_{1-x} alloy films have been grown on Si(100) substrates by cosputtering from pure Si and Co targets so that alloy composition may be selected by varying the relative power of each target, as reported elsewhere.[36] The Co_xSi_{1-x} films are polycrystalline for high Co content but become amorphous below $x=0.75$ as checked by high angle x-ray diffraction. The detailed structural characterization of Co_xSi_{1-x} films by x-ray absorption spectroscopy and surface x-ray diffraction[37,38] has shown that the amorphization process takes place in a gradual way as a function of Co content: as Si atoms are introduced in the alloy structure there is a coexistence of amorphous and polycrystalline areas with reduced grain size until long-range order disappears below $x=0.75$. In the amorphous films, only short-range order is observed with a certain degree of clustering of Co atoms.[37]

The Nb layers have also been grown by sputtering[24,31] on top of the magnetic alloy films. The Nb deposition has been performed in a single run to avoid small changes in the superconducting properties related with different conditions during growth. The magnetic and superconducting layer thicknesses are kept constant in all the series ($d_F=40$ nm and $d_S=25$ nm) so that all the observed changes can be related to the variation in magnetic properties of the alloy films, and not to the thickness dependence of proximity effect.[21] It is worth to mention that possible structural and/or magnetic changes in the ferromagnetic/nonmagnetic layer as a function of thickness can have a direct influence on the bilayer T_C, such as has been reported in Nb/Fe[4] and Nb/Pd systems.[39] Keeping d_F constant allows us to discard this factor in data analysis. The value $d_F=40$ nm has been chosen so that it is larger than typical values of ξ_F length even for weak ferromagnets ($\xi_F \approx 1-15$ nm).[7,12,13,20,21,23,27,30,40] Thus, we can make the initial assumption that the bilayers are in the thick layer limit and the proximity effect is saturated. The validity of this hypothesis will be revised later in Sec. IV.

Magnetic and superconducting properties of the *a*-Co_xSi_{1-x} films and *a*-Co_xSi_{1-x}/Nb bilayers have been characterized by superconducting quantum interference device magnetometry and magnetotransport measurements with a standard four-point method in a He cryostat with a 90 kOe superconducting magnet. The results of this characterization for a single 25 nm Nb film grown on Si(100) as a control sample for the bilayers are low-temperature resistivity $\rho_S(10\ \mathrm{K})=25\ \mu\Omega$ cm and superconducting critical temperature $T_{CS}=6.1\pm0.1$ K (obtained from the midpoint of the resistivity transition), which are typical of Nb films in this thickness range.[41] The electronic mean-free path in the Nb can be obtained as[41] $l_{Nb}=3.72\times10^{-6}\ \mu\Omega\ \mathrm{cm}^2/\rho_S=1.5$ nm, which indicates that the Nb film is in the dirty limit. The superconducting coherence length is given by

$$\xi_S = \sqrt{\frac{\hbar D_S}{2\pi k_B T_{CS}}}, \tag{1}$$

where D_S is the diffusion coefficient in the superconductor $D_S=v_{Nb}l_{Nb}/3=1.33\ \mathrm{cm}^2/\mathrm{s}$ and $v_{Nb}=2.73\times10^7$ cm/s is the Fermi velocity in Nb.[42] Thus, with the above values $\xi_S=5.2$ nm. The upper critical field is $H_{c2}(0)=40.5$ kOe, obtained from the field dependence of the resistivity transitions. Thus, the Ginzburg-Landau coherence length can be calculated as[43] $\xi_{GL}=\sqrt{\frac{\Phi_0}{2\pi H_{c2}}}=9$ nm which, in turn, allows us to estimate ξ_S length as $\xi_S=\frac{2}{\pi}\xi_{GL}=5.7$ nm in good agreement with the results of Eq. (1).

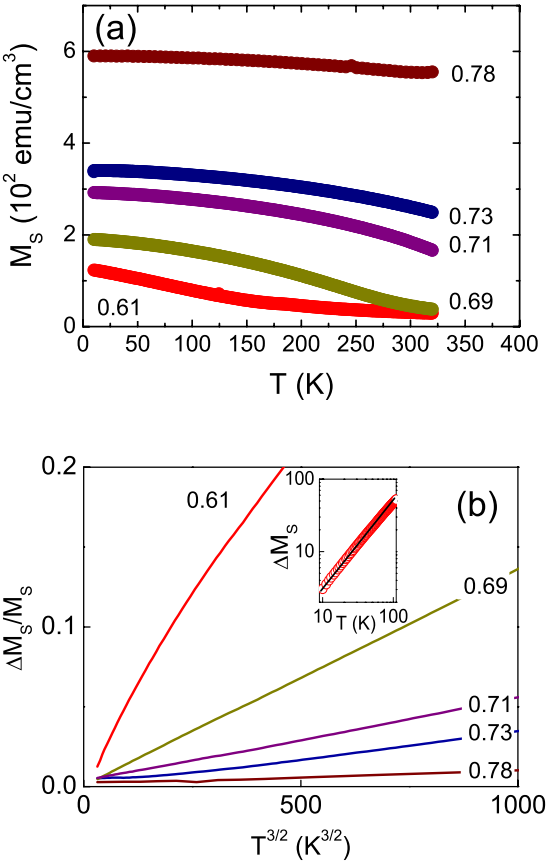

FIG. 1. (Color online) (a) Temperature dependence of the saturation magnetization of a series of Co_xSi_{1-x} alloy films. (b) Low-temperature dependence of $\Delta M_S/M_S=[M_S(0)-M_S(T)]/M_S(0)$ vs $T^{3/2}$. Note the deviations of the $x=0.61$ film from the linear behavior predicted by the Bloch law. Labels indicate Co content x for each curve. Inset is a log-log plot of ΔM_S vs T for the $x=0.61$ film showing a low-temperature linear dependence with a reduced exponent. Solid line is a linear fit.

III. RESULTS AND DISCUSSION

A. Magnetic properties of Co_xSi_{1-x} films

Figure 1(a) shows the temperature dependence of the saturation magnetization M_S of a series of Co_xSi_{1-x} alloy films with $x=0.61-0.78$, measured in a constant magnetic field of 400 Oe. As Co content is reduced the overall values of M_S become lower and, also, a stronger temperature dependence $M_S(T)$ is observed. This reveals the gradual loss of magnetic character and the reduction in the Curie temperature of the alloy as the magnetic atoms become more diluted: for $x<0.7$ the Curie temperature falls below room temperature, in agreement with previous results[36,44] and, finally,

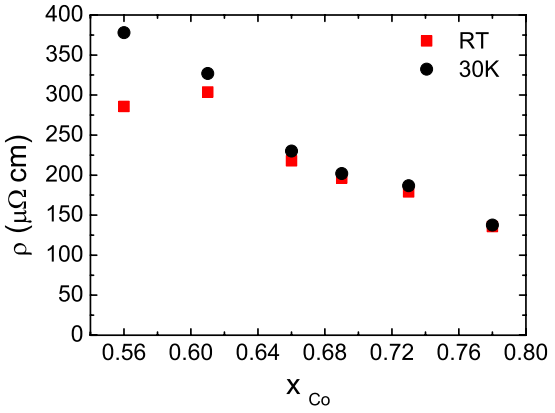

FIG. 2. (Color online) Resistivity as a function of Co content for a series of Co_xSi_{1-x} alloy films measured at room temperature (squares) and at 30 K (circles).

magnetism is completely lost at any temperature, within the measurement resolution, for a sample with $x=0.56$ (not included in Fig. 1). As shown in Fig. 1(b), the $M_S(T)$ curves follow well the typical $T^{3/2}$ Bloch law for x above 0.69. $M_S(T)$ can be fitted[45] to $[M_S(0)-M_S(T)]=BT^{3/2}$ with $B=5.22\mu_B[k_B/4\pi D_{sw}]^{3/2}$, where μ_B is the Bohr magneton, k_B the Boltzmann constant, and D_{sw} the spin-wave stiffness constant. D_{sw} values obtained from the fit of the curves in Fig. 1(b) vary from 100 meV Å^2 for $x=0.69$ to 280 meV Å^2 for $x=0.78$, which are equivalent to reported values for Co-Si-B amorphous alloys with a similar Co content.[45] However, for the sample with $x=0.61$, i.e., with a composition just above the threshold for ferromagnetic behavior, the corresponding $[M_S(0)-M_S(T)]$ vs $T^{3/2}$ curve is no longer a straight line [see Fig. 1(b)], indicating a different temperature behavior. At low T, below 100 K, $[M_S(0)-M_S(T)]$ can be fitted to a Bloch law with a reduced exponent. $[M_S(0)-M_S(T)]\propto T^{1.1}$ [see inset in Fig. 1(b)] and $M_S(T)$ presents a concave upward curvature in a wide temperature range. This behavior cannot be understood within a simple model of a homogeneous magnetic material; rather, this $M_S(T)$ shape is characteristic of strong fluctuations in the exchange field[46] and of granular magnetic materials.[47] These could be related with the short-range composition fluctuations typical of transition-metal-metalloid glasses[48] due to the differences in bonding between the different kinds of atoms present in the alloy. Actually, in these amorphous Co-Si alloys, the nanosegregation of two Co-rich and Si-rich intermixed phases has already been observed for high Si content[37,49] with a typical length scale on the order of 5 nm.

Transport mechanisms in disordered metal-metalloid alloys[50–52] can be quite different than in the crystalline and polycrystalline ferromagnetic materials mostly used in proximity effect experiments.[30] Figure 2 shows the resistivity of a series of Co_xSi_{1-x} alloy films as a function of Co content x measured at room temperature (squares) and at 30 K (circles). Resistivity values are rather large and for almost all the samples ρ lies above the Mooij criterion for weak localization ($\rho \geq 150$ $\mu\Omega$ cm).[53] ρ increases gradually as x is reduced without any significant feature at $x=0.75$, when the samples become amorphous. This is in agreement with previous results[49] and with the gradual character of the amorphization process observed in the structural characterization of these alloys.[38] The temperature coefficient of resistance, $\beta=d\log\rho/dT$ is close to zero for $x>0.64$ and becomes negative as the transition to the nonmagnetic amorphous phase is approached $\beta\approx-10^{-3}$ K^{-1} and -2×10^{-4} K^{-1} for $x=0.56$ and $x=0.61$, respectively. In the framework of Ziman theory of liquid metals extended to disordered alloys,[54] a change in sign in the temperature coefficient of resistivity is related to the position of the first peak in the x-ray structure factor relative to the Fermi wave vector. In magnetic amorphous alloys[45,50] this behavior has also been attributed to weak localization effects.

The dirty limit ferromagnetic coherence length ξ_F^* is defined as

$$\xi_F^* = \sqrt{\frac{\hbar D_F}{2\pi k_B T_{CS}}}, \tag{2}$$

where D_F is the diffusion coefficient in the ferromagnetic layer. This can be derived from the resistivity values in the amorphous alloy using the Einstein relation[50]

$$1/\rho = e^2 N(E_F) D_F, \tag{3}$$

where e is the electron charge and $N(E_F)$ is the density of states at the Fermi level. The density of states[55] in pure Co is $N(E_F)_{Co}=1.1\times10^{48}$ J^{-1} m^{-3}. However, in Co-based magnetic amorphous alloys (such as Co-B, Co-B-Si, and Co-Zr-Si) an increase in $N(E_F)$ has been reported as Co content is reduced caused by a decrease in the exchange splitting between Co majority and minority bands upon introduction of metalloid atoms in the structure,[45,56] i.e., as magnetism is weakened in the alloys. An empirical correlation was established between the specific-heat coefficient and the spin-wave stiffness constant for a variety of Co-based amorphous samples. In particular, in the range $D_{sw}\approx100-300$ meV Å^{-2} corresponding to the *a*-Co-Si films used in this work, the specific-heat coefficient was found to be approximately constant and 30% higher than that of pure Co. Thus, we have taken as a first approximation $N(E_F)_{Co\text{-}Si}=1.3N(E_F)_{Co}$. Then, in the studied composition range, ξ_F^* length is found to vary in an almost linear way from 1.2 nm for the $Co_{0.56}Si_{0.54}$ sample up to $\xi_F^*=2$ nm for the $Co_{0.78}Si_{0.22}$ film.

B. Superconducting properties of Co_xSi_{1-x}/Nb bilayers

The resistive transitions $R(T)$ of several Co_xSi_{1-x}/Nb bilayers can be seen in Fig. 3(a), normalized by the normal-state resistance just above the transition, R_N. All the samples exhibit sharp superconducting transitions of width $\Delta T=T(0.9R_N)-T(0.1R_N)\approx0.1$ K. The curves are displaced to lower temperatures as Co content x increases, until the nonmagnetic amorphous phase is reached and the transition temperature increases back again. This can be seen in more detail in Fig. 3(b) in which the midpoint transition temperatures $T_C=T(0.5R_N)$ have been plotted as a function of Co composition. For high x, the bilayer transition temperatures are close to that of a single Nb film of the same thickness $T_{CS}=6.1$ K and follow a decreasing trend down to $T_C=5.2$ K at

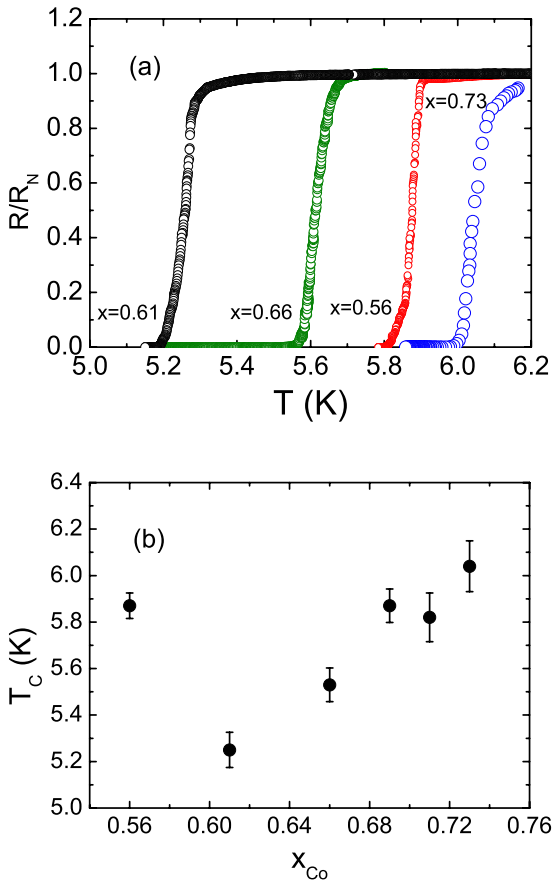

FIG. 3. (Color online) (a) Resistive transitions normalized respect to the normal-state resistance R_N for several Co_xSi_{1-x}/Nb bilayers. Labels indicate Co content x for each curve. (b) Superconducting transition temperatures of the Co_xSi_{1-x}/Nb bilayers as a function of Co content x. Error bars indicate $0.1R_N-0.9R_N$ transition widths.

$x=0.61$. In any case, the observed proximity effect induced by the amorphous Co_xSi_{1-x} layers is rather weak, with a maximum change in T_C of less than 15% of T_{CS}, indicating a short penetration of the Cooper pairs into the disordered magnetic alloy.

IV. ANALYSIS OF THE DATA AND DISCUSSION

Proximity effect between superconducting and ferromagnetic materials is usually described within the framework of the linearized Usadel equations[15,21,23] with the appropriate boundary conditions. Theoretical models considering homogeneous ferromagnetic layers have been successfully applied to analyze the experimental behavior of different S/F systems, in terms of different material parameters. Only very recently, the role of disorder in the ferromagnetic layer has been considered from a theoretical point of view.[32,33] Thus, the analysis of the proximity effect data in the Co_xSi_{1-x}/Nb bilayers will be performed in two steps: first, the data will be discussed in terms of "homogeneous ferromagnet proximity models"[15,21,23] in order to make a direct comparison with previous experiments in the literature[23,30,57] and, then, this analysis will be revised adding the effect of disorder as calculated by recent theoretical works.[32,33]

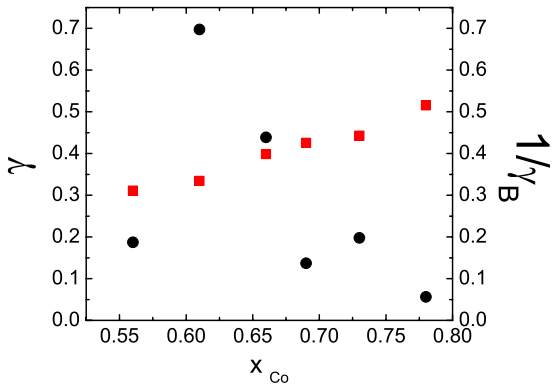

FIG. 4. (Color online) Proximity effect parameters in the Co_xSi_{1-x}/Nb bilayers as a function of Co content in the alloy: γ (squares) and $1/\gamma_b$ (circles).

A. Homogenous ferromagnet models

In the dirty limit, within a single mode approximation, the transition temperature of a S/F bilayer T_C is given by[21]

$$\psi\left(\frac{1}{2}+\Omega^2\frac{T_{CS}}{2T_C}\right)-\psi\left(\frac{1}{2}\right)=\ln\left(\frac{T_{CS}}{T_C}\right),$$

$$\Omega\tan\left(\Omega\frac{d_S}{\xi_S}\right)=\frac{\gamma}{\gamma_b} \tag{4}$$

where ψ is the digamma function, Ω is the real root of Eq. (4), and γ_b and γ are the parameters that characterize interface resistance and the strength of the proximity effect, respectively. γ is given by[21]

$$\gamma=\frac{\rho_S\xi_S}{\rho_F\xi_F^*} \tag{5}$$

so that in the Co_xSi_{1-x} films, it can be calculated from the results in Sec. III A. γ is found to increase monotonously as a function of Co content from $\gamma=0.3$ to 0.5 as x varies from 0.56 to 0.78 (see squares in Fig. 4). The parameter γ_b is directly related to interface transparency,[30] Tr, $[\gamma_b\propto(1-Tr)/Tr]$ so that a low value of γ_b corresponds to a transparent interface while a large γ_b is indicative of large interface resistance and low transparency. In the limit of weak T_C suppression, as is the case here, Eq. (4) can be further simplified as[21]

$$1-\frac{T_C}{T_{CS}}\approx\frac{\pi^2\xi_S}{4d_S}\frac{\gamma}{\gamma_b}, \tag{6}$$

allowing us to estimate the composition dependence of γ_b directly from the T_C vs x data (see circles in Fig. 4). $1/\gamma_b$ presents a nonmonotonous x dependence: as the Co content is reduced, $1/\gamma_b$ increases smoothly from $1/\gamma_b\approx0.1$ for the film with the highest Co content ($x=0.78$) and reaches a maximum $1/\gamma_b\approx0.7$ for $x=0.61$ (i.e., the sample with the lowest Co content that is still ferromagnetic); then,

for the nonmagnetic $Co_{56}Si_{44}$/Nb sample, $1/\gamma_b$ decreases again down to $1/\gamma_b \approx 0.2$. It is interesting to check now the applicability of the single mode approximation[21] in this system: for thick enough magnetic layers ($d_F \gg \xi_F^*$ as is the case here), Eq. (4) holds as long as $1/\gamma_b \ll \max[\sqrt{T_C/T_{CS}}, \sqrt{E_{ex}/(\pi k_B T_{CS})}]$ with E_{ex} the exchange energy in the ferromagnet. Taking into account that $1/\gamma_b$ is always smaller that unity, this criterion implies either a Curie temperature above $\pi T_{CS} \approx 20$ K (which is clearly fulfilled for all the magnetic alloys with $x > 0.6$) or $1/\gamma_b \ll \sqrt{T_C/T_{CS}}$ which is also fulfilled by the $x=0.56$ sample.

In spite of the very different conduction mechanisms in crystalline and noncrystalline materials, the results are qualitatively in agreement with previous works on the superconducting proximity effects with polycrystalline ferromagnets: interface transparency is very low for strong ferromagnets [$1/\gamma_b = 0.012$ and $1/\gamma_b = 0.025$ have been reported for V/Fe (Ref. 23) and Nb/Fe (Ref. 57)] whereas much larger values are found for weak ferromagnets such as Pd-Ni alloys[30] with Curie temperature around 150 K ($1/\gamma_b = 1.6$). Also, in V/Fe_xV_{1-x} multilayers,[23] interface transparency was found to decrease monotonously as a function of Fe content. Thus, there could be some additional factor in the observed general trend of an enhanced proximity effect for alloy based weak ferromagnets.

B. Role of disorder in the inhomogenous ferromagnet model

The theoretical model used above[21] corresponds to a homogeneous ferromagnet and does not take into account the possibility of inhomogeneities in the magnetic layer. This is hardly the case for these amorphous Co_xSi_{1-x} alloys in view of the results of the magnetic characterization. In particular, the sample $Co_{0.61}Si_{0.39}$, with the strongest T_C reduction, is the one that shows a $M_S(T)$ curve characteristic of a granular ferromagnetic material. Very recently,[32,33] it has been shown that magnetic disorder with arbitrary correlation length can be incorporated as a local spin-flip term Γ_{sf} in the Usadel equations. In these amorphous materials, the electron mean-free path becomes on the order of interatomic distances,[50] which is shorter than the length scale for composition fluctuations in these films (about 5 nm), implying that these samples are in a nonlocal regime. In this case, $\Gamma_{sf} \sim (\delta h)^2 a^2 / D_F$, with δh the fluctuating exchange field due to magnetic disorder and a the typical size of the correlated magnetic regions.[33] Then, for a S/F bilayer with a thick enough magnetic layer, spin-flip scattering modifies the proximity effect by a ferromagnet with a homogeneous exchange energy E_{ex} (and homogeneous exchange field h) described in Eq. (6) as[22]

$$1 - \frac{T_C}{T_{CS}} \approx \frac{\pi^2 \xi_S}{4 d_S} \frac{\gamma}{\gamma_b} \left(1 - \frac{\alpha}{2 \widetilde{d_F} \tilde{\gamma}} \right), \tag{7}$$

where $\alpha \sim \Gamma_{sf}/h$, $\widetilde{d_F} = d_F/\xi_F$, and $\tilde{\gamma} = \gamma_b \xi_F^*/\xi_F$. In the dirty limit,[22,30] $\xi_F = \sqrt{\hbar D_F / E_{ex}} \sim \sqrt{D_F/h}$. Thus, in the thick ferromagnetic layer limit, magnetic disorder actually weakens the proximity effect by the homogeneous ferromagnet, resulting in an effective reduction in the $1/\gamma_b$ values estimated from Eq. (6). This could explain in part the weak T_C suppression observed in Fig. 3 for the samples with the highest Co content.

On the other hand, for the thin magnetic layer case, the effect of magnetic scattering changes sign, and enhances the T_C suppression by the homogeneous exchange field as

$$\left[1 - \frac{T_C}{T_{CS}} \right]_\alpha \approx \left[1 - \frac{T_C}{T_{CS}} \right]_{\alpha=0} \left(1 + \frac{2\alpha}{\widetilde{d_F} \tilde{\gamma}} \right). \tag{8}$$

The limit condition between these two regimes for a S/F bilayer is given by[22] $2\widetilde{d_F}\tilde{\gamma} = 1$, which translates into the equivalent condition for the ferromagnetic layer thickness

$$d_F = \frac{\xi_F^2}{2 \gamma_b \xi_F^*}. \tag{9}$$

It is important to note that the dirty limit ξ_F diverges as the material looses its magnetic character. Thus, for a fixed d_F, as Co content x is reduced and the transition to a nonmagnetic phase is approached, the condition given by Eq. (9) will be reached at some point. Then, the effect of magnetic disorder will change sign, resulting in a stronger T_C suppression [and a larger effective value of $1/\gamma_b$ as given by Eq. (6)]. In the present case, according to Eq. (9), the Co-Si sample with $x = 0.61$ will fall out of the thick layer regime as long as $\xi_F > 12$ nm, which is not an unreasonable value in view of the low saturation magnetization of this sample. Therefore, magnetic disorder described by a spin-flip scattering term into the Usadel equations,[22,33] reinforces the expected T_C vs x dependence associated to an enhancement of interface transparency for the less magnetic alloys[21,23] and can give an additional contribution for the observe T_C minimum at the boundary between the magnetic and nonmagnetic amorphous phases.

V. CONCLUSIONS

In summary, the magnetic and superconducting properties of *a*-Co_xSi_{1-x}/25 nm Nb bilayers have been studied as a function of Co content x. As the Co atoms become more diluted disorder increases in the magnetic alloy, as indicated by the presence of a negative temperature coefficient of resistance β and a change in the temperature dependence of the saturation magnetization that deviates from the $T^{3/2}$ bulk Bloch law, which could be caused by strong fluctuations in the exchange field.

The critical temperature reduction in the Nb layers due to proximity effect with the Co_xSi_{1-x} layer is weak, indicating a short penetration of the Cooper pairs in the amorphous magnetic alloys. The superconducting T_C is gradually suppressed as x decreases and the lowest T_C value appears at $x=0.61$, the composition just above the alloy looses its ferromagnetic character, which can be understood in terms of an enhanced interface transparency and/or an increase in the spin-flip scattering term due to the magnetic inhomogeneities in the sample.

ACKNOWLEDGMENTS

Work supported by Spanish MICINN (Grants No. FIS2008-06249, No. HP2008-0032, and Consolider No. CSD2007-00010), CAM under Grant No. S2009/MAT-1726, UCM-Santander under Grant No. GR58-08, Asturias FICYT (IB08-106 and BP06-109), and CRUP of Portugal (Grant No. E41/09) in the framework of the Spanish-Portuguese Integrated Action. G.N.K. acknowledges support from FCT of Portugal through the "Ciencia 2007" program. We acknowledge L. Fernandez-Seivane for help with data acquisition software.

*mvelez@uniovi.es

[1] A. I. Buzdin, Rev. Mod. Phys. **77**, 935 (2005).
[2] C. Strunk, C. Sürgers, U. Paschen, and H. v. Löhneysen, Phys. Rev. B **49**, 4053 (1994).
[3] J. S. Jiang, D. Davidovic, D. H. Reich, and C. L. Chien, Phys. Rev. Lett. **74**, 314 (1995).
[4] Th. Mühge, N. N. Garif'yanov, Yu. V. Goryunov, G. G. Khaliullin, L. R. Tagirov, K. Westerholt, I. A. Garifullin, and H. Zabel, Phys. Rev. Lett. **77**, 1857 (1996).
[5] L. V. Mercaldo, C. Attanasio, C. Coccorese, L. Maritato, S. L. Prischepa, and M. Salvato, Phys. Rev. B **53**, 14040 (1996).
[6] G. Verbanck, C. D. Potter, V. Metlushko, R. Schad, V. V. Moshchalkov, and Y. Bruynseraede, Phys. Rev. B **57**, 6029 (1998).
[7] L. Lazar, K. Westerholt, H. Zabel, L. R. Tagirov, Yu. V. Goryunov, N. N. Garif'yanov, and I. A. Garifullin, Phys. Rev. B **61**, 3711 (2000).
[8] V. Peña, Z. Sefrioui, D. Arias, C. Leon, J. Santamaría, M. Varela, S. J. Pennycook, and J. L. Martínez, Phys. Rev. B **69**, 224502 (2004).
[9] S. Luo, T. Crozes, B. Gilles, S. Rajauria, B. Pannetier, and H. Courtois, Phys. Rev. B **79**, 140508(R) (2009).
[10] M. Vélez, J. I. Martín, J. E. Villegas, A. Hoffmann, E. M. González, J. L. Vicent, and I. K. Schuller, J. Magn. Magn. Mater. **320**, 2547 (2008).
[11] J. Xia, V. Shelukhin, M. Karpovski, A. Kapitulnik, and A. Palevski, Phys. Rev. Lett. **102**, 087004 (2009).
[12] V. Zdravkov, A. Sidorenko, G. Obermeier, S. Gsell, M. Schreck, C. Müller, S. Horn, R. Tidecks, and L. R. Tagirov, Phys. Rev. Lett. **97**, 057004 (2006).
[13] A. Potenza and C. H. Marrows, Phys. Rev. B **71**, 180503(R) (2005).
[14] G. X. Miao, A. V. Ramos, and J. S. Moodera, Phys. Rev. Lett. **101**, 137001 (2008).
[15] Z. Radović, M. Ledvij, L. Dobrosavljević-Grujić, A. I. Buzdin, and J. R. Clem, Phys. Rev. B **44**, 759 (1991).
[16] M. G. Khusainov and Yu. N. Proshin, Phys. Rev. B **56**, R14283 (1997).
[17] E. A. Demler, G. B. Arnold, and M. R. Beasley, Phys. Rev. B **55**, 15174 (1997).
[18] K. Halterman and O. T. Valls, Phys. Rev. B **65**, 014509 (2001).
[19] F. S. Bergeret, A. F. Volkov, and K. B. Efetov, Phys. Rev. Lett. **86**, 4096 (2001).
[20] A. Bagrets, C. Lacroix, and A. Vedyayev, Phys. Rev. B **68**, 054532 (2003).
[21] Ya. V. Fominov, N. M. Chtchelkatchev, and A. A. Golubov, Phys. Rev. B **66**, 014507 (2002).
[22] M. Fauré, A. I. Buzdin, A. A. Golubov, and M. Yu. Kupriyanov, Phys. Rev. B **73**, 064505 (2006).
[23] J. Aarts, J. M. E. Geers, E. Brück, A. A. Golubov, and R. Coehoorn, Phys. Rev. B **56**, 2779 (1997).
[24] M. Vélez, C. Martínez, A. Cebollada, F. Briones, and J. L. Vicent, J. Magn. Magn. Mater. **240**, 580 (2002).
[25] I. A. Garifullin, D. A. Tikhonov, N. N. Garif'yanov, M. Z. Fattakhov, L. R. Tagirov, K. Theis-Bröhl, K. Westerholt, and H. Zabel, Phys. Rev. B **70**, 054505 (2004).
[26] H. Yamazaki, N. Shannon, and H. Takagi, Phys. Rev. B **73**, 094507 (2006).
[27] K. Kim, J. H. Kwon, J. Kim, K. Char, H. Doh, and H.-Y. Choi, Phys. Rev. B **74**, 174503 (2006).
[28] A. Potenza, M. S. Gabureac, and C. H. Marrows, J. Appl. Phys. **103**, 07C703 (2008).
[29] E. Navarro, M. Vélez, Y. Huttel, A. Pérez-Junquera, J. I. Martín, O. F. de Lima, A. Cebollada, J. M. Alameda, and J. L. Vicent, J. Appl. Phys. **105**, 033912 (2009).
[30] C. Cirillo, S. L. Prischepa, M. Salvato, C. Attanasio, M. Hesselberth, and J. Aarts, Phys. Rev. B **72**, 144511 (2005).
[31] M. Vélez, M. C. Cyrille, S. Kim, J. L. Vicent, and I. K. Schuller, Phys. Rev. B **59**, 14659 (1999).
[32] J. Linder, T. Yokoyama, and A. Sudbø, Phys. Rev. B **79**, 054523 (2009).
[33] D. A. Ivanov, Ya. V. Fominov, M. A. Skvortsov, and P. M. Ostrovsky, Phys. Rev. B **80**, 134501 (2009).
[34] J. W. A. Robinson, J. D. S. Witt, and M. G. Blamire, Science **329**, 59 (2010).
[35] C. Bell, S. Turşucu, and J. Aarts, Phys. Rev. B **74**, 214520 (2006).
[36] M. Vélez, C. Meny, S. M. Valvidares, J. Díaz, R. Morales, L. M. Alvarez-Prado, and J. M. Alameda, Eur. Phys. J. B **41**, 517 (2004).
[37] J. Díaz, R. Morales, S. M. Valvidares, and J. M. Alameda, Phys. Rev. B **72**, 144413 (2005).
[38] C. Quirós, L. Zárate, J. Díaz, P. Prieto, J. Rubio-Zuazo, and J. M. Alameda, J. Phys.: Condens. Matter **19**, 486003 (2007).
[39] A. Potenza, M. S. Gabureac, and C. H. Marrows, Phys. Rev. B **76**, 014534 (2007).
[40] A. Angrisani Armenio, C. Cirillo, G. Iannone, S. L. Prischepa, and C. Attanasio, Phys. Rev. B **76**, 024515 (2007).
[41] M. S. M. Minhaj, S. Meepagala, J. T. Chen, and L. E. Wenger, Phys. Rev. B **49**, 15235 (1994).
[42] H. R. Kerchner, D. K. Christen, and S. T. Sekula, Phys. Rev. B **24**, 1200 (1981).
[43] M. Tinkham, *Introduction to Superconductivity* (Mc Graw-Hill, New York, 1975).
[44] S. Giron, Ph.D. thesis, Universidad Complutense de Madrid, 1986.
[45] U. Mizutani, M. Hasegawa, K. Fukamichi, Y. Hattori, Y. Yamada, H. Tanaka, and S. Takayama, Phys. Rev. B **47**, 2678 (1993).

[46] For a review on amorphous alloys see, e.g., M. E. McHenry, M. A. Willard, and D. E. Laughlin, Prog. Mater. Sci. **44**, 291 (1999).
[47] D. Zhang, K. J. Klabunde, C. M. Sorensen, and G. C. Hadjipanayis, Phys. Rev. B **58**, 14167 (1998).
[48] C. Hausleitner and J. Hafner, Phys. Rev. B **47**, 5689 (1993).
[49] J. M. Fallon, C. A. Faunce, and P. J. Grundy, J. Phys.: Condens. Matter **12**, 4075 (2000).
[50] N. Mott, *Conduction in Non-Crystalline Materials* (Clarendon Press, Oxford, 1993).
[51] A. Möbius, C. Frenzel, R. Thielsch, R. Rosenbaum, C. J. Adkins, M. Schreiber, H. D. Bauer, R. Grötzschel, V. Hoffmann, T. Krieg, N. Matz, H. Vinzelberg, and M. Witcomb, Phys. Rev. B **60**, 14209 (1999).
[52] J. Sonntag, Phys. Rev. B **71**, 115114 (2005); **40**, 3661 (1989).
[53] J. H. Mooij, Phys. Status Solidi A **17**, 521 (1973).
[54] P. J. Cote and L. V. Meisel, Phys. Rev. Lett. **39**, 102 (1977).
[55] C. Kittel, *Introduction to Solid State Physics* (Wiley, New York, 1996).
[56] H. Tanaka, S. Takayama, M. Hasegawa, T. Fukunaga, U. Mizutani, A. Fujita, and K. Fukamichi, Phys. Rev. B **47**, 2671 (1993).
[57] J. M. E. Geers, M. B. S. Hesselberth, J. Aarts, and A. A. Golubov, Phys. Rev. B **64**, 094506 (2001).